Enhanced indistinguishability of in-plane single photons by resonance fluorescence on an integrated quantum dot

Sokratis Kalliakos[1,], Yarden Brody[1,2], Anthony J. Bennett[1], David J. P. Ellis[1], Joanna Skiba-Szymanska[1], Ian Farrer[2], Jonathan P. Griffiths[2], David A. Ritchie[2], and Andrew J. Shields[1]*

[1] Cambridge Research Laboratory, Toshiba Research Europe Limited, 208 Science Park, Milton Road, Cambridge, CB4 0GZ, United Kingdom

[2] Cavendish Laboratory, University of Cambridge, J. J. Thomson Avenue, Cambridge CB3 0HE, United Kingdom.

ABSTRACT Integrated quantum light sources in photonic circuits are envisaged as building blocks of future on-chip architectures for quantum logic operations. While semiconductor quantum dots have been proven to be highly efficient emitters of quantum light, their interaction with the host material induces spectral decoherence, which decreases the indistinguishability of the emitted photons and limits their functionality. Here, we show that the indistinguishability of in-plane photons can be greatly enhanced by performing resonance fluorescence on a quantum dot coupled to a photonic crystal waveguide. We find that the resonant optical excitation of an exciton state induces an increase of the emitted single-photon coherence by a factor of 15. Two-photon interference experiments reveal a visibility of 0.80 ± 0.03, which is good agreement with

our theoretical model. Combined with the high in-plane light-injection efficiency of photonic crystal waveguides, our results pave the way for the use of this system for on-chip generation and transmission of highly indistinguishable photons.

The proposal to perform quantum computation operations using only single photons and linear optics has motivated significant scientific efforts.[1] Within this scheme, an essential building block is a source that is able to emit single and indistinguishable photons with high efficiency. The performance of semiconductor quantum dots (QDs) as integrated quantum-light emitters has been very promising for on-chip applications and integration in photonic quantum circuits.[2] Using optical excitation or electrical carrier injection, single QDs have proven to be excellent single-photon[3–5] and entangled photon-pair emitters.[6,7]

At the heart of the proposed protocols for two-qubit gates in linear optics quantum computation lies the interference of single-photon pulses on a beam splitter. Perfect two-photon interference (TPI) visibility can only be achieved when the two interfering photons are indistinguishable in terms of polarization, frequency, bandwidth and arrival times at the beam splitter. Even though emission of indistinguishable photons has been demonstrated using QDs,[8–10] the interaction of the carriers in the QD with the host semiconductor matrix has a detrimental effect on the coherence time of the emitted photons, which essentially limits indistinguishability. It has been shown that under optical off-resonant and quasi-resonant (*p*-shell) excitation conditions, single-photon coherence is limited by the electrostatic fluctuations in the QD environment and incoherent phonon-related relaxation mechanisms to the ground state.[8,11,12] The photon coherence time T_2 is highly dominated by the dephasing time T^*_2 (loss of coherence before the photon emission) through the relation $1/T_2 = 1/(2T_1) + 1/T^*_2$, with T_1 being the radiative lifetime. In the absence of dephasing effects, the emitted single-photon pulses are Fourier transform-limited and $T_2 = 2T_1$. Dephasing effects can be greatly suppressed by direct *s*-shell optical excitation and collection of highly-coherent photons has therefore been achieved by resonance fluorescence (RF).[13–20] The major challenge in these experiments is the rejection of laser light, which is usually achieved using cross-polarization techniques. Using RF, photon indistinguishabilities close to unity have been reported.[17,19]

The vast majority of RF experiments on QDs are restricted to the emission of light out of the plane of the semiconductor chip. However, in the emerging field of photonic quantum information technology, it is highly desirable for the integrated quantum emitter to be able to emit highly indistinguishable photons into an on-chip quantum circuit. The integration of QDs in photonic circuits, in particular photonic crystal waveguides (PCWGs),[21–27] has extended the use of these emitters as integrated in-plane quantum light sources. These systems offer broadband operation,[20] efficiency[23,28] and scalability.[27] Recently, the in-plane emission of indistinguishable photons from a PCWG under non-resonant excitation has been demonstrated.[29]

There have been several recent attempts to use resonant excitation schemes in order to enhance the coherence properties of in-plane photons.[30–32] All of the experiments have been performed in ridge GaAs waveguides containing In(Ga)As QDs. Enhancement of the photon coherence time has been observed, as well as sub-Poissonian statistics for in-plane photons. In addition, out-of-plane single photons have been generated from a QD strongly coupled to a photonic crystal cavity under resonant excitation.[33] In this case, spectral detuning of the QD with respect to the cavity mode allowed for efficient stray light rejection by spectrally filtering light from the cavity mode. On the other hand, there have been no reports yet of RF in photonic crystal structures, presumably due to difficulties in stray laser light rejection. In this letter, we report the in-plane emission of highly-indistinguishable photons generated by RF on a QD coupled to a PCWG. Compared to non-resonant optical excitation conditions, the RF-induced in-plane photons show an increase in coherence time by a factor of 15. We show that this enhancement has a direct impact on in-plane photon indistinguishability by measuring a maximum TPI visibility of 80%, limited by experimental imperfections.

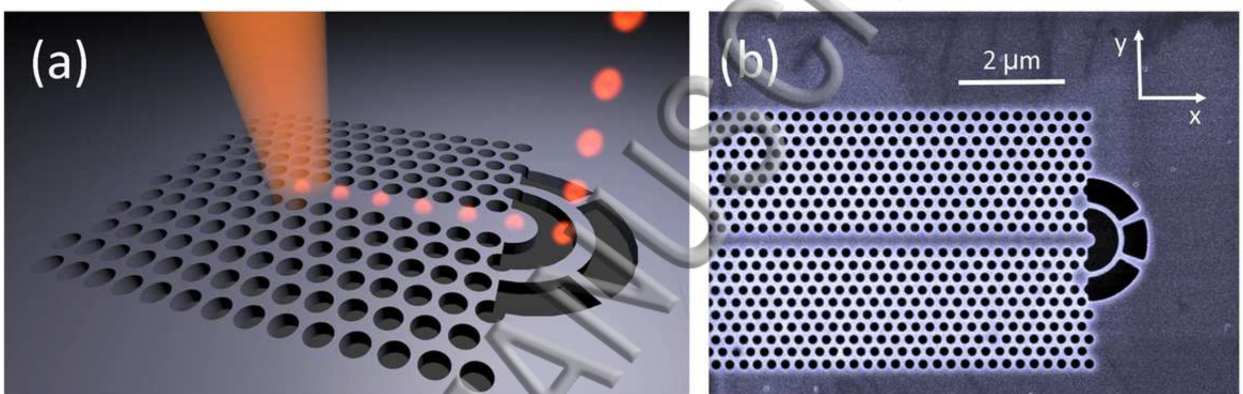

Figure 1. (a) Schematic illustration of the PCWG and the operating principle of the experiment. A linearly-polarized laser in resonance with the QD state excites the QD in the waveguiding region of a PCWG. Cross-polarized photons are transmitted along the waveguide and scatter out of the plane from the out-coupling grating. (b) Scanning electron microscope image of a PCWG with an out-coupling grating.

Our system for the generation and transmission of in-plane photons consists of a GaAs unidirectional PCWG slab with a layer of low-density InAs in the middle of the slab. In order to collect the in-plane photons, we added an out-coupling grating at the exit of the waveguide.[34] Its parameters were chosen in order to vertically scatter photons with a frequency matching the *y*-

polarized fundamental propagation mode of the waveguide.[29] A graphic illustration of the principle of the experiment is shown in Fig. 1(a) and a scanning electron microscope image of the device is shown in Fig. 1(b). A tunable continuous wave (CW) laser polarized along the *x*-axis resonantly excites an excitonic transition in a QD coupled to the PCWG. *y*-polarized photons generated by RF are transmitted along the waveguide and are scattered vertically by the out-coupling grating. The polarization configuration of the excitation and emitted light implies that the excitonic state in the QD is a charged state.[35] The spatial separation of the excitation and collection spots, together with their orthogonal polarizations allows us to achieve an RF signal to stray laser light ratio of ~ 15.

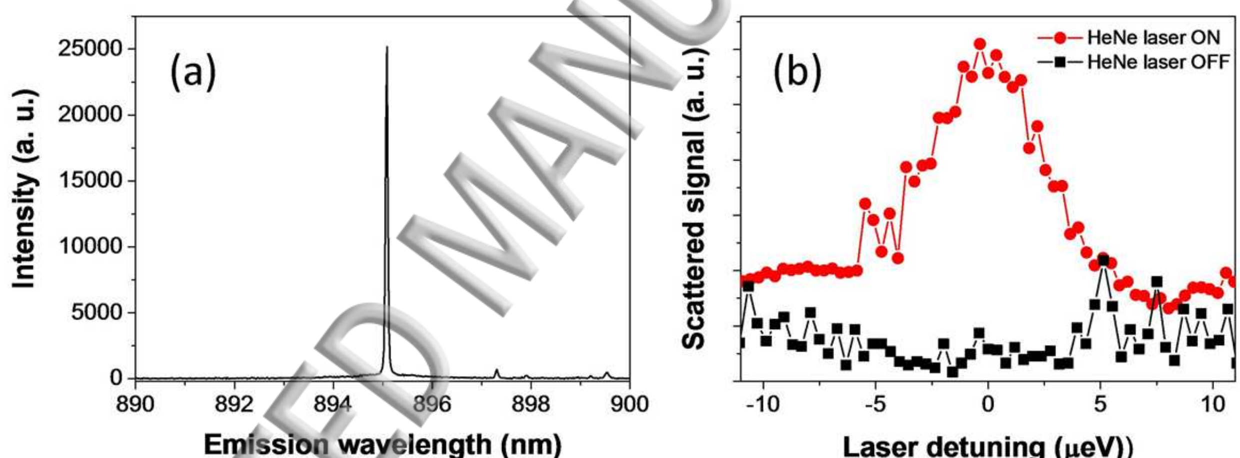

Figure 2. (a) In-plane emission spectrum from a QD in a PCWG under above band gap pulse excitation. (b) In-plane resonance fluorescence signal as a function of laser detuning from the QD state with the weak off-resonant HeNe laser on (red line) and off (black line).

The in-plane spectrum from a QD excited by a non-resonant pulsed laser (λ = 780 nm) is shown in Fig. 2(a). The spectrum is dominated by an intense peak at 895.1 nm, attributed to a charged excitonic recombination from a QD. It is difficult to precisely determine the efficiency of the out-coupling grating but the detected count rates in this case are comparable to previous reports where the in-plane emission was collected directly from the exit of the waveguide.[23,29] Calculations of the photonic band structure of an infinite PCWG using the plane-wave expansion method with the same parameters as the one used in the experiment show spectral matching of the emission at 895.1 nm with the fundamental y-polarized propagating mode.[29]

Fig. 2(b) shows the in-plane RF signal as a function of CW laser detuning. In order to be able to observe RF, a second, very weak non-resonant illumination from an attenuated laser (HeNe, λ = 633 nm) for above-band gap excitation was used in order to stabilize the fluctuating electrostatic environment in the vicinity of the QD.[20,31] The contribution of the QD photoluminescence caused by the off-resonant illumination to the total detected count rates was less than 0.5%. Strong enhancement of the detected signal is observed when the tunable laser is on resonance with the excitonic transition of the QD (red line). A Gaussian fitting indicates a full width at half maximum (FWHM) of 6 μeV, which corresponds to a T_2 of ~ 700 ps. However, as we show next, this value is underestimated, most probably due to spectral diffusion that causes an increase of the measured linewidth of the transition. The RF signal vanishes when the off-resonant illumination is turned off (black line in Fig. 2(b)).

The in-plane single-photon coherence time was measured using a Michelson interferometer. A measure of the first-order correlation function is given by the photon interference visibility as a function of the relative time delay between the two arms of the interferometer. In the case of above band gap non-resonant excitation, the in-plane single-photon coherence time is measured to be 94 ± 4 ps (Fig. 3(a), blue squares), severely limited by the decoherence mechanisms described above. Keeping the count rates at the same level (~ 50 Kcounts/s), the coherence time of in-plane RF photons is 1.47 ± 0.18 ns (black squares), a dramatic 15-fold increase. Time-resolved photoluminescence measurements using an off-resonant pulsed laser diode reveal a QD emission lifetime T_1 = 0.70 ± 0.03 ns, which indicates that the in-plane RF emitted photons are close to the Fourier-transform limited case. The errors in the experimentally-extracted values have been determined using the least-squares fitting method.

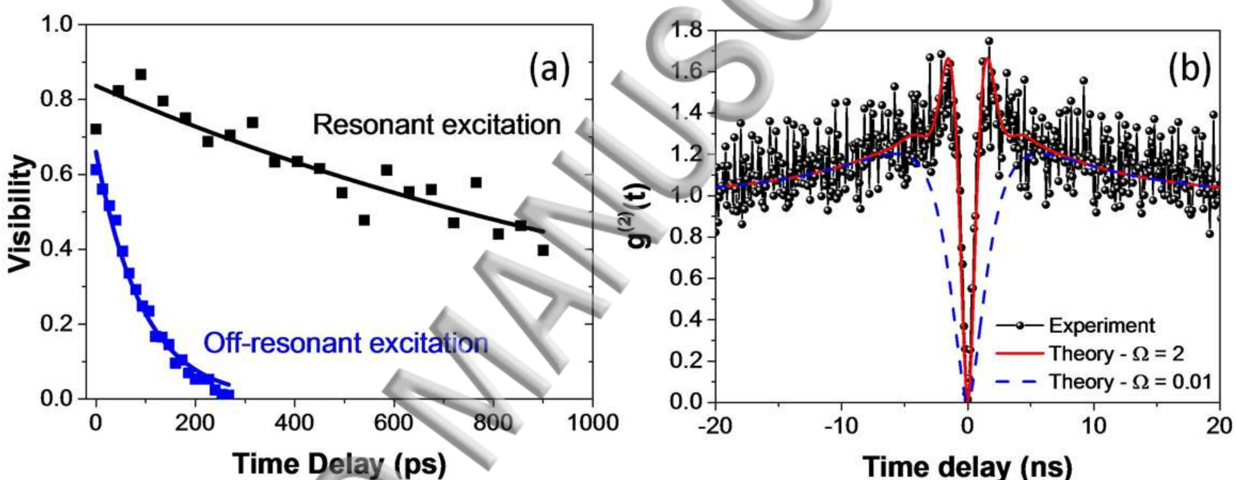

Figure 3. (a) Single-photon interference visibility as a function of the relative time delay between the two arms of a Michelson interferometer. Black (blue) squares refer to measurements under resonant (non-resonant) excitation conditions. Thick lines are exponential fits. (b) Second-order correlation function of in-plane single photons emitted by RF. The thick red line is the result of our model with a Rabi parameter Ω = 2, where the dashed blue line is the result of the same model with Ω = 0.01.

The quantum nature of the in-plane emitted light was confirmed by performing autocorrelation measurements using a fiber-based Hanbury Brown and Twiss set up. For light detection, we used superconducting single-photon detectors (SSPDs) that allow us to achieve a high time resolution (100 ps). The second-order correlation function of in-plane RF photons is shown in Fig. 3(b). Contributions due to stray laser light (~ 6%) have been subtracted and the coincidences have been averaged over a time bin of 100 ps.[36] A pronounced dip at $t = 0$ is observed, with $g^{(2)}(0) = 0.02 \pm 0.02$ (raw data 0.10 ± 0.02). For longer positive and negative time delays, photon bunching is present with a characteristic time of 8 ns. Such an effect is commonly seen in resonant excitation experiments and is usually attributed to charge-related effects[37] and/or the interaction of the QD state with the nuclear spins in the local environment.[38] We used a previously developed model[39] for CW coherent excitation in QDs in order to reproduce our experimental data. The critical parameters are the measured emission lifetime and coherence time $T_1 = 0.70$ ns and $T_2 = 1.47$ ns, respectively, as well as the Rabi parameter Ω that is related to the Rabi frequency. Under resonant excitation conditions, the second-order correlation function $g^{(2)}(t)$ is given by:

$$g^{(2)}(t) = 1 - \left[\cos(\beta t) + \frac{\alpha}{\beta}\sin(\beta t)\right] e^{-\alpha t} \tag{1}$$

where $\alpha = \frac{1}{2}(\frac{1}{T_1} + \frac{1}{T_2})$ and $\beta = \sqrt{\Omega^2 - \frac{1}{4}(\frac{1}{T_1} - \frac{1}{T_2})^2}$. The bunching effect has been included using an exponential decay with characteristic time constant $T_b = 8$ ns.. At low excitation condition (with Rabi parameter $\Omega = 0.01$, which corresponds to $0.01 \cdot (2\pi)^{-1}$ Rabi cycles/ns), the model fails to reproduce the experimental $g^{(2)}(t)$ (Fig. 3(b), blue dashed line), in particular the strong bunching observed at short positive and negative time delays (at $t = \pm 1.5$ ns). On the other hand, a good agreement is achieved when we introduce a higher Rabi parameter $\Omega = 2$ (which corresponds to $2 \cdot (2\pi)^{-1}$ Rabi cycles/ns, Fig. 3(b), red line). This is a direct confirmation of the

RF origin of the in-plane photons. We stress that, even if the resonant character of the excitation has a direct impact on the second-order correlation function, the Rabi frequency is small (Ω = 2, Rabi frequency ~ 0.3 GHz) to induce beating effects in the first-order correlation data (Fig. 3(a)) within our time scale. This consistent with the single-photon interference visibilities calculated using the model described above.[39]

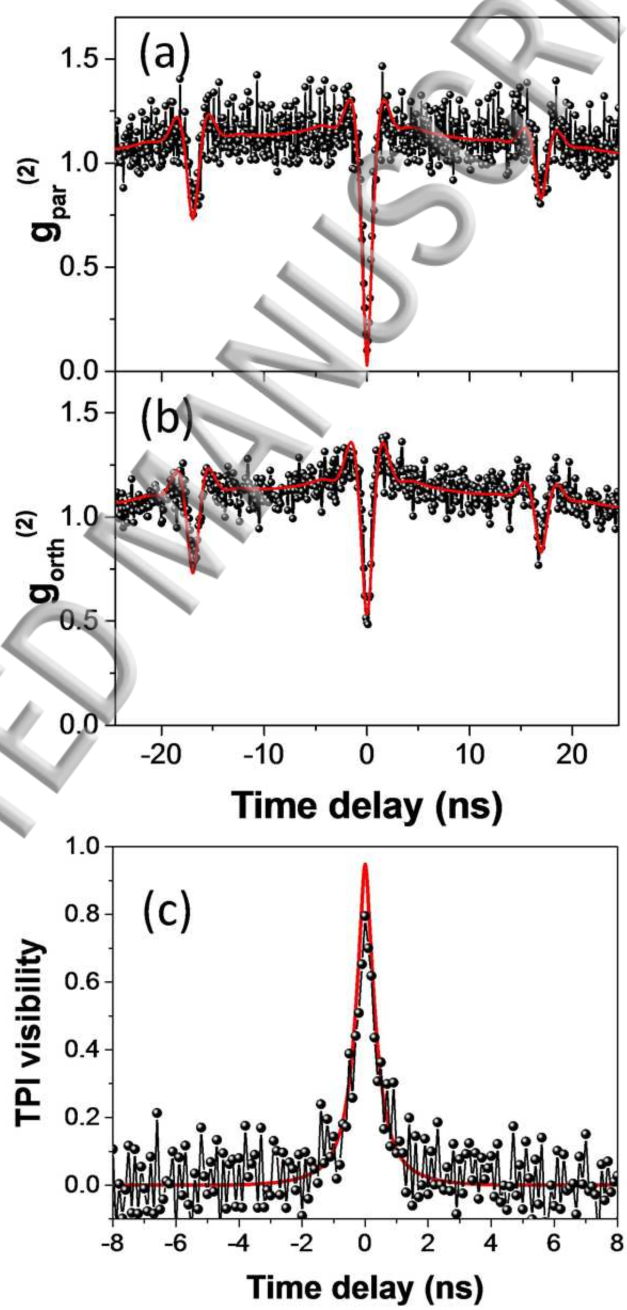

Figure 4. (a) Second-order correlation function of cross-polarized interfering photons emitted in-plane by RF. (b) Second-order correlation function of co-polarized interfering photons emitted in-plane by RF. (c) TPI visibility as a function of time delay for in-plane photons emitted by RF. The red lines in all panels is the result of our model with a Rabi parameter $\Omega = 2$.

We confirmed the enhanced indistinguishability of in-plane single photons emitted by RF by performing TPI using a polarization-maintaining fiber-based Mach-Zehnder interferometer.[29] An optical delay line of 16.9 ns was introduced in one arm of the interferometer, while the other arm contained an in-line polarization controller. The delay line was chosen to be much longer than the photon coherence time to prevent lower-order interference effects. The total count rates were kept at ~ 40 Kcounts/s. The second-order correlation function for the case of orthogonal and parallel-polarized interfering photons is shown in Fig. 4(a) and 4(b), respectively. The experimental data have been corrected for background contributions.[36] For a perfect single-photon source, antibunched correlations at $t = 0$ occur 50% of the time when the photons are distinguishable (orthogonal polarization in the two arms of the interferometer). This is what we observe in Fig. 4(a), with $g_{\mathrm{orth}}^{(2)}(0) = 0.49 \pm 0.02$ (raw data 0.53 ± 0.01). In the case of indistinguishable interfering photons (same polarization set in both paths), destructive interference will occur at the second beam splitter for photon arrival times falling within the photon coherence time. This causes photon bunching at the beamsplitter and a pronounced antibunching in the coincidence events recorded by the detectors. The second-order correlation function for co-polarized interfering photons is shown in Fig. 4(b) with $g_{\mathrm{par}}^{(2)}(0) = 0.10 \pm 0.01$ (raw data 0.18 ± 0.01). The degree of the in-plane photon indistinguishability is defined by the TPI visibility, which is given by $V(t) = (g_{\mathrm{orth}}^{(2)}(t) - g_{\mathrm{par}}^{(2)}(t)) / g_{\mathrm{orth}}^{(2)}(t)$. This post-selective measurement is valid since the temporal resolution of our set up is much shorter than the photon coherence time. In the case of photon detectors with temporal resolution comparable or longer than the photon coherence time, the photon indistinguishability is measured by the coalescence time window, as has been shown recently.[40] The TPI visibility under RF as a function of time delay is shown in Fig. 4(c). The highest visibility is achieved at $t = 0$ and is found to be $V(0) = 0.80 \pm 0.03$ (raw data 0.66 ± 0.04). Such a high visibility is the direct consequence of the resonant emission mechanism and the enhanced photon coherence time. The excitation mechanism has also a strong influence on the width of the visibility peak, shown in Fig. 4(c). When fitted with a Lorentzian function, the FWHM is 0.87 ± 0.06 ns. This is a 5-fold improvement over the previously reported value of 0.16 ns for in-plane photon emission under off-resonant excitation.[29]

The theoretical curves (thick red lines) in Fig. 4 have been calculated using the following formulas:[41]

$$g^{(2)}_{orth}(t) = 4(T_A^2 + R_A^2)R_B T_B g^{(2)}(t) + 4R_A T_A\left[T_B^2 g^{(2)}(t - \Delta\tau_2) + R_B^2 g^{(2)}(t + \Delta\tau_2)\right] \tag{2}$$

$$g^{(2)}_{par}(t) = 4(T_A^2 + R_A^2)R_B T_B g^{(2)}(t) + 4R_A T_A\left[T_B^2 g^{(2)}(t - \Delta\tau_2) + R_B^2 g^{(2)}(t + \Delta\tau_2)\right] \times \left(1 - Fe^{-2\frac{|t|}{T_2}}\right) \tag{3}$$

where T_A (R_A) and T_B (R_B) are the transmission (reflection) coefficients of the first and second fiber beam splitters, respectively and F is a function that depends on the overlap of the wave functions at the second fiber beam splitter. In our calculations we have set $F = 1$. The parameters used are $T_1 = 0.70$ ns, $T_2 = 1.47$ ns, $\Delta\tau_2 = 16.9$ ns, transmission and reflection coefficients of the beamsplitters $T_A = T_B = 0.55$ and $R_A = R_B = 0.45$, respectively. A good agreement between experiment and theory is achieved. In particular, the enhanced width of the TPI visibility peak is reproduced, confirming the role of the long coherence time achieved by RF. Our model predicts a TPI visibility of 0.94, close to the value we measured experimentally. Deviations of the experimental value from the predicted TPI visibility is mainly attributed to the instability of our cryogenic set-up, which may induce changes in the ratio of RF signal to stray laser light over the time of the experiment. In addition, the photon polarization in the arms of the interferometer could only be set with an accuracy of ~ 95%, which would affect the detected correlations of interfering (or not interfering) photons. Improvements on the mechanical stability of our cryogenic system together with the use of minimal-error optical elements should allow future studies to demonstrate perfect indistinguishability of in-plane photons using PCWGs.

In conclusion, we have demonstrated the in-plane emission of indistinguishable photons generated by RF on a QD coupled to a PCWG. The resonant excitation mechanism allowed us to observe a 15-fold increase in the coherence time of photons emitted along the plane of the chip when compared to above-band gap excitation. The long coherence time has a dramatic impact on the photon indistinguishability, which was demonstrated by the measured TPI visibility of 0.80 ± 0.03. Theoretical models of RF on QDs developed previously provide a good agreement with our experimental findings. Our results highlight the potential of QDs embedded in PCWGs as sources of highly-indistinguishable in-plane photons. Given the high efficiency of these systems for in-plane photon injection,[22] the possibility to perform RF in PCWG structures paves the way for the integration of quantum light sources with high photon indistinguishability in sophisticated quantum photonic integrated circuit architectures.

Aknowledgements

We acknowledge support by the Marie Curie Actions within the Seventh Framework Programme for Research of the European Commission, under the Initial Training Network PICQUE (Grant No. 608062). The Engineering and Physical Sciences Research Council (EPSRC) partly funded the molecular beam epitaxy machine used to grow the sample.

Author information

Corresponding Author

* E–mail: sokratis.kalliakos@crl.toshiba.co.uk

Present Addresses

I. F: Department of Electronic & Electrical Engineering, The University of Sheffield, Mappin Street, Sheffield, S1 3JD, U.K.

References

[1] E. Knill, R. Laflamme, and G.J. Milburn, Nature **409**, 46 (2001).
[2] A.J. Shields, Nat. Photonics **1**, 215 (2007).
[3] P. Michler, A. Kiraz, C. Becher, W.V. Schoenfeld, P.M. Petroff, L. Zhang, E. Hu, and A. Imamoglu, Science **290**, 2282 (2000).
[4] S. Strauf, N.G. Stoltz, M.T. Rakher, L.A. Coldren, P.M. Petroff, and D. Bouwmeester, Nat. Photonics **1**, 704 (2007).
[5] Z. Yuan, B.E. Kardynal, R.M. Stevenson, A.J. Shields, C.J. Lobo, K. Cooper, N.S. Beattie, D.A. Ritchie, and M. Pepper, Science **295**, 102 (2002).
[6] R.M. Stevenson, R.J. Young, P. Atkinson, K. Cooper, D.A. Ritchie, and A.J. Shields, Nature **439**, 179 (2006).
[7] C.L. Salter, R.M. Stevenson, I. Farrer, C.A. Nicoll, D.A. Ritchie, and A.J. Shields, Nature **465**, 594 (2010).
[8] C. Santori, D. Fattal, J. Vučković, G.S. Solomon, and Y. Yamamoto, Nature **419**, 594 (2002).
[9] R.B. Patel, A.J. Bennett, I. Farrer, C.A. Nicoll, D.A. Ritchie, and A.J. Shields, Nat. Photonics **4**, 632 (2010).
[10] S. Laurent, S. Varoutsis, L.L. Gratiet, A. Lemaître, I. Sagnes, F. Raineri, A. Levenson, I. Robert-Philip, and I. Abram, Appl. Phys. Lett. **87**, 163107 (2005).
[11] A. Kiraz, M. Atatüre, and A. Imamoğlu, Phys. Rev. A **69**, 32305 (2004).
[12] A.J. Bennett, D.C. Unitt, A.J. Shields, P. Atkinson, and D.A. Ritchie, Opt. Express **13**, 7772 (2005).

[13] A. Muller, E.B. Flagg, P. Bianucci, X.Y. Wang, D.G. Deppe, W. Ma, J. Zhang, G.J. Salamo, M. Xiao, and C.K. Shih, Phys. Rev. Lett. **99**, 187402 (2007).
[14] S. Ates, S.M. Ulrich, S. Reitzenstein, A. Löffler, A. Forchel, and P. Michler, Phys. Rev. Lett. **103**, 167402 (2009).
[15] A. Ulhaq, S. Weiler, S.M. Ulrich, R. Roßbach, M. Jetter, and P. Michler, Nat. Photonics **6**, 238 (2012).
[16] C. Matthiesen, A.N. Vamivakas, and M. Atatüre, Phys. Rev. Lett. **108**, 93602 (2012).
[17] Y.-M. He, Y. He, Y.-J. Wei, D. Wu, M. Atatüre, C. Schneider, S. Höfling, M. Kamp, C.-Y. Lu, and J.-W. Pan, Nat. Nanotechnol. **8**, 213 (2013).
[18] A.V. Kuhlmann, J. Houel, A. Ludwig, L. Greuter, D. Reuter, A.D. Wieck, M. Poggio, and R.J. Warburton, Nat. Phys. **9**, 570 (2013).
[19] X. Ding, Y. He, Z.-C. Duan, N. Gregersen, M.-C. Chen, S. Unsleber, S. Maier, C. Schneider, M. Kamp, S. Höfling, C.-Y. Lu, and J.-W. Pan, Phys. Rev. Lett. **116**, (2016).
[20] A.J. Bennett, J.P. Lee, D.J.P. Ellis, T. Meany, E. Murray, F.F. Floether, J.P. Griffths, I. Farrer, D.A. Ritchie, and A.J. Shields, Sci. Adv. **2**, e1501256 (2016).
[21] T. Lund-Hansen, S. Stobbe, B. Julsgaard, H. Thyrrestrup, T. Sünner, M. Kamp, A. Forchel, and P. Lodahl, Phys. Rev. Lett. **101**, 113903 (2008).
[22] E. Viasnoff-Schwoob, C. Weisbuch, H. Benisty, S. Olivier, S. Varoutsis, I. Robert-Philip, R. Houdré, and C.J.M. Smith, Phys. Rev. Lett. **95**, 183901 (2005).
[23] A. Schwagmann, S. Kalliakos, I. Farrer, J.P. Griffiths, G.A.C. Jones, D.A. Ritchie, and A.J. Shields, Appl. Phys. Lett. **99**, 261108 (2011).
[24] A. Schwagmann, S. Kalliakos, D.J.P. Ellis, I. Farrer, J.P. Griffiths, G.A.C. Jones, D.A. Ritchie, and A.J. Shields, Opt. Express **20**, 28614 (2012).
[25] T.B. Hoang, J. Beetz, M. Lermer, L. Midolo, M. Kamp, S. Höfling, and A. Fiore, Opt. Express **20**, 21758 (2012).
[26] A. Laucht, S. Pütz, T. Günthner, N. Hauke, R. Saive, S. Frédérick, M. Bichler, M.-C. Amann, A.W. Holleitner, M. Kaniber, and J.J. Finley, Phys. Rev. X **2**, 11014 (2012).
[27] A. Jamil, J. Skiba-Szymanska, S. Kalliakos, A. Schwagmann, M.B. Ward, Y. Brody, D.J.P. Ellis, I. Farrer, J.P. Griffiths, G.A.C. Jones, D.A. Ritchie, and A.J. Shields, Appl. Phys. Lett. **104**, 101108 (2014).
[28] P. Yao, V. s. c. Manga Rao, and S. Hughes, Laser Photonics Rev. **4**, 499 (2010).
[29] S. Kalliakos, Y. Brody, A. Schwagmann, A.J. Bennett, M.B. Ward, D.J.P. Ellis, J. Skiba-Szymanska, I. Farrer, J.P. Griffiths, G.A.C. Jones, D.A. Ritchie, and A.J. Shields, Appl. Phys. Lett. **104**, 221109 (2014).
[30] M. Schwartz, U. Rengstl, T. Herzog, M. Paul, J. Kettler, S.L. Portalupi, M. Jetter, and P. Michler, Opt. Express **24**, 3089 (2016).
[31] M.N. Makhonin, J.E. Dixon, R.J. Coles, B. Royall, I.J. Luxmoore, E. Clarke, M. Hugues, M.S. Skolnick, and A.M. Fox, Nano Lett. **14**, 6997 (2014).
[32] G. Reithmaier, M. Kaniber, F. Flassig, S. Lichtmannecker, K. Müller, A. Andrejew, J. Vučković, R. Gross, and J.J. Finley, Nano Lett. **15**, 5208 (2015).
[33] D. Englund, A. Majumdar, A. Faraon, M. Toishi, N. Stoltz, P. Petroff, and J. Vučković, Phys. Rev. Lett. **104**, 73904 (2010).
[34] A. Faraon, I. Fushman, D. Englund, N. Stoltz, P. Petroff, and J. Vuckovic, Opt. Express **16**, 12154 (2008).
[35] A.B. Young, A.C.T. Thijssen, D.M. Beggs, P. Androvitsaneas, L. Kuipers, J.G. Rarity, S. Hughes, and R. Oulton, Phys. Rev. Lett. **115**, 153901 (2015).

[36] See supplemental material at [URL will be inserted by AIP] for the background subtraction method, (n.d.).
[37] C. Santori, D. Fattal, J. Vučković, G.S. Solomon, E. Waks, and Y. Yamamoto, Phys. Rev. B **69**, 205324 (2004).
[38] J. Hansom, C.H.H. Schulte, C. Le Gall, C. Matthiesen, E. Clarke, M. Hugues, J.M. Taylor, and M. Atatüre, Nat. Phys. **10**, 725 (2014).
[39] H.S. Nguyen, G. Sallen, C. Voisin, P. Roussignol, C. Diederichs, and G. Cassabois, Phys Rev Lett **108**, 57401 (2012).
[40] R. Proux, M. Maragkou, E. Baudin, C. Voisin, P. Roussignol, and C. Diederichs, Phys. Rev. Lett. **114**, 67401 (2015).
[41] R.B. Patel, A.J. Bennett, K. Cooper, P. Atkinson, C.A. Nicoll, D.A. Ritchie, and A.J. Shields, Phys Rev Lett **100**, 207405 (2008).

Figure Captions

Figure 1. (a) Schematic illustration of the PCWG and the operating principle of the experiment. A linearly-polarized laser in resonance with the QD state excites the QD in the waveguiding region of a PCWG. Cross-polarized photons are transmitted along the waveguide and scatter out of the plane from the out-coupling grating. (b) Scanning electron microscope image of a PCWG with an out-coupling grating.

Figure 2. (a) In-plane emission spectrum from a QD in a PCWG under above band gap pulse excitation. (b) In-plane resonance fluorescence signal as a function of laser detuning from the QD state with the weak off-resonant HeNe laser on (red line) and off (black line).

Figure 3. (a) Single-photon interference visibility as a function of the relative time delay between the two arms of a Michelson interferometer. Black (blue) squares refer to measurements under resonant (non-resonant) excitation conditions. Thick lines are exponential fits. (b) Second-order correlation function of in-plane single photons emitted by RF. The thick red line is the result of our model with a Rabi parameter $\Omega = 2$, where the dashed blue line is the result of the same model with $\Omega = 0.01$.

Figure 4. (a) Second-order correlation function of cross-polarized interfering photons emitted in-plane by RF. (b) Second-order correlation function of co-polarized interfering photons emitted

in-plane by RF. (c) TPI visibility as a function of time delay for in-plane photons emitted by RF. The red lines in all panels is the result of our model with a Rabi parameter $\Omega = 2$.

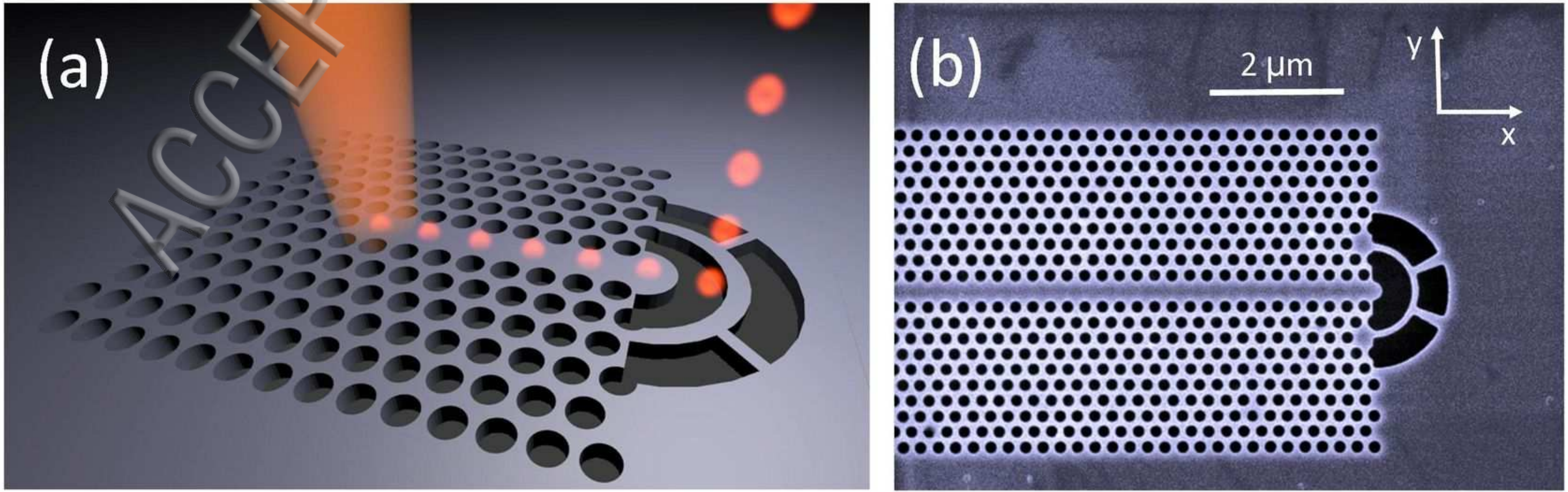

(a)
(b)
2 μm
y
x

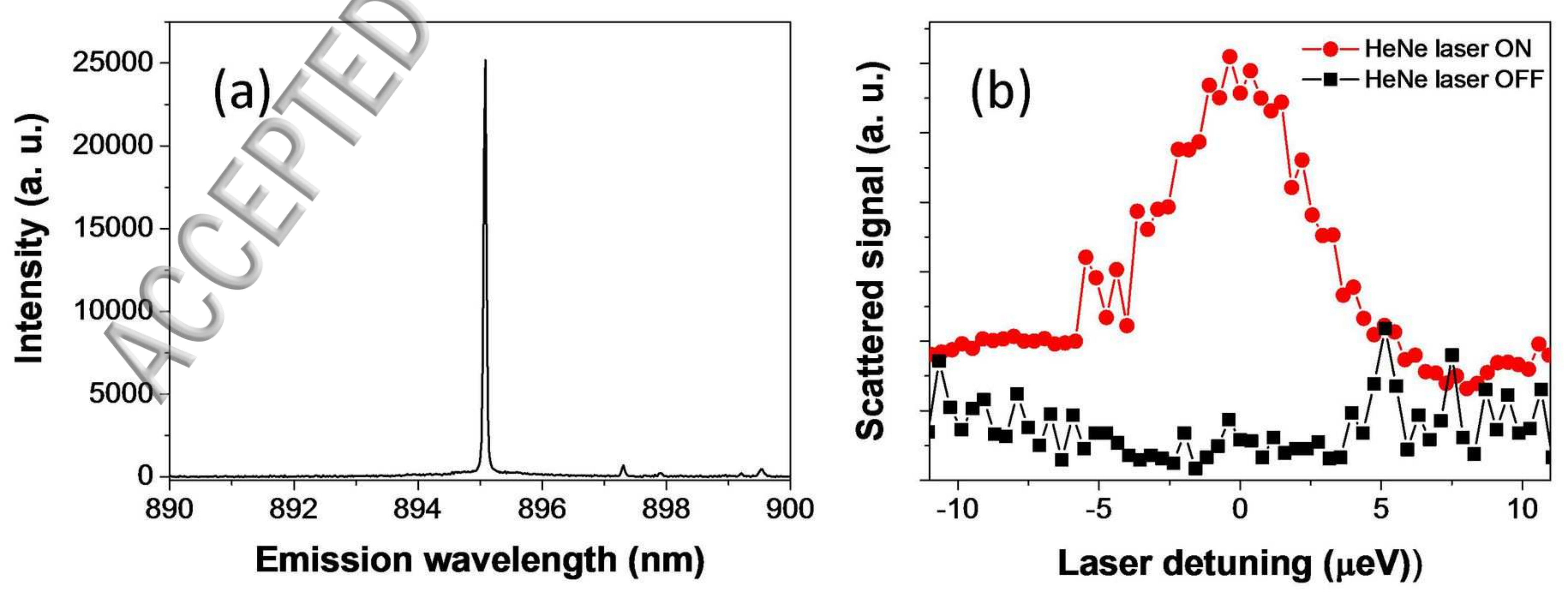
(a)
Intensity (a. u.)
25000
20000
15000
10000
5000
0
890
892
894
896
898
900
Emission wavelength (nm)
(b)
HeNe laser ON
HeNe laser OFF
Scattered signal (a. u.)
-10
-5
0
5
10
Laser detuning (μeV))

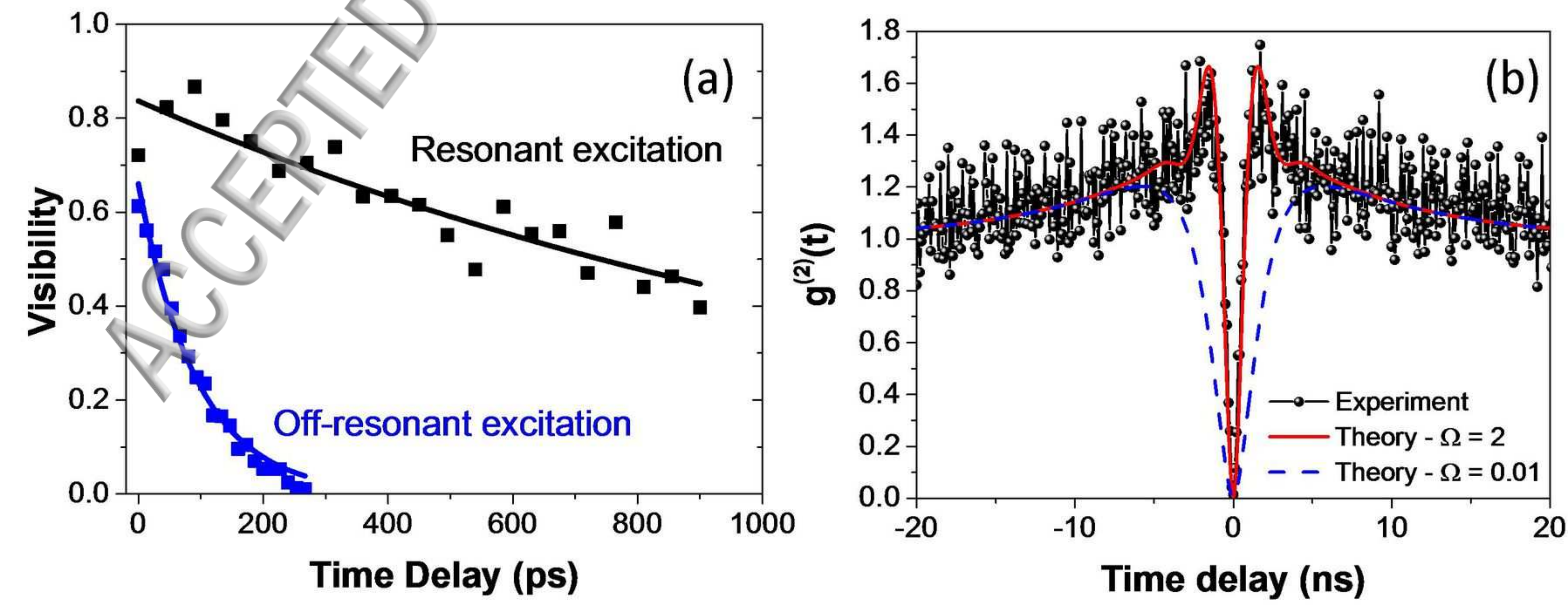

(a)
Resonant excitation
Off-resonant excitation
Visibility
Time Delay (ps)
0.0
0.2
0.4
0.6
0.8
1.0
0
200
400
600
800
1000
(b)
$g^{(2)}(t)$
Time delay (ns)
0.0
0.2
0.4
0.6
0.8
1.0
1.2
1.4
1.6
1.8
-20
-10
0
10
20
Experiment
Theory - Ω = 2
Theory - Ω = 0.01

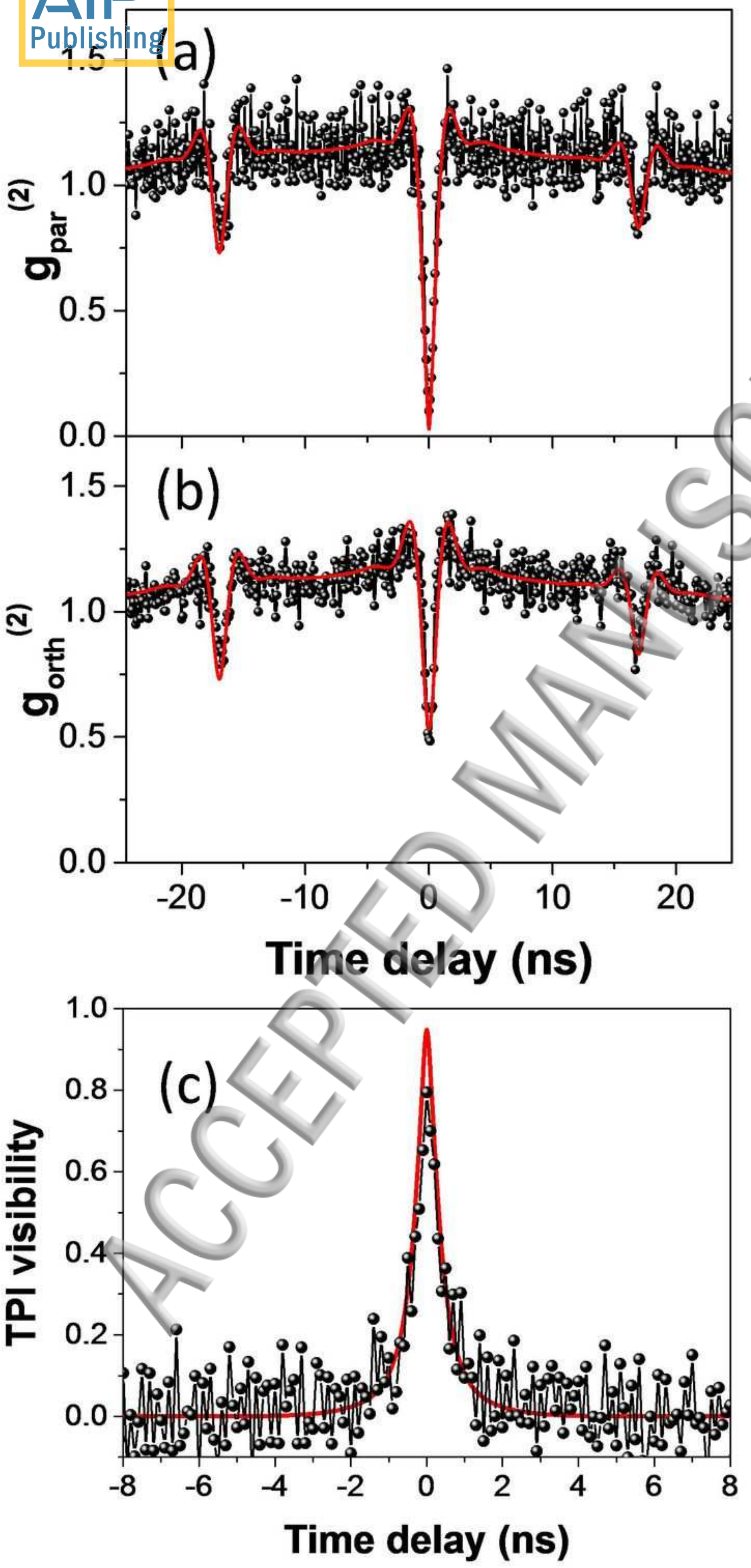

(a)
(b)
(c)
1.5
1.0
0.5
0.0
$g^{(2)}_{par}$
$g^{(2)}_{orth}$
-20
-10
0
10
20
Time delay (ns)
1.0
0.8
0.6
0.4
0.2
0.0
TPI visibility
-8
-6
-4
-2
0
2
4
6
8
Time delay (ns)